Temperature Distribution in the Force-Driven Poiseuille Gas Flow by Molecular Dynamics

Ravichandran RANJITH [1], Jae Hyun PARK [1,2], Rho Shin MYONG [1,2,*]

* Corresponding author: Tel.: +82-55-772-1645; Fax: +82-55-772-1580; Email: myong@gnu.ac.kr
1 Department of Aerospace and System Engineering, Gyeongsang National University, South Korea
2 Department of Aerospace and System Engineering and Research Center for Aircraft Parts Technology, Gyeongsang National University, South Korea

Abstract The thermal behavior of the force-driven compressible Poiseuille gas flow is studied by molecular dynamics (MD) simulation method. This type of flow situation occurs in the cooling system of MEMS/NEMS devices and hence the properties of Poiseuille gas flow become significant, especially the thermal behavior. The peculiar behavior of the force-driven Poiseuille gas flow, local minimum at the center in the temperature profile, is investigated in detail. Emphasis is placed on variations of the temperature distribution for different Knudsen numbers. Previously, the central temperature minimum and other flow peculiarities have been described by a non-classical non-Fourier theory based on nonlinear coupled constitutive relations. The main goal of this study is to investigate the thermal behavior of the force-driven Poiseuille gas flow using molecular dynamics simulations and to compare the results with that of non-classical non-Fourier theory. The MD results in general show agreement with the data from the non-classical hydrodynamic theory, which confirms the validity of MD method in analyzing the micro/nano gas flows including thermal behaviors.

Keywords: force-driven Poiseuille flow, thermal behavior, molecular dynamics (MD), non-Fourier law

1. Introduction

The flow behaviors of the micro/nano gas flows are of great interest to researchers since there is a fundamental question whether the continuum (macroscopic) theories can describe such flows. The results predicted by the classical hydrodynamic theories for Poiseuille gas flows at macroscopic scale are quite different from that of the flows at micro/nano scales. In this regard, the thermo-physical properties of micro/nano channel flows are important due to the fact that these flow types find their applications in the cooling system of MEMS/NEMS devices. Moreover, they help in estimating the transport properties of a fluid (Prabha and Sathian, 2013) and calculating accommodation coefficients (Prabha and Sathian, 2012), slip length, and so on.

Compressible Poiseuille gas flow is a well-known benchmark flow problem in which the fluid is confined between two infinitely long parallel plates, and the fluid is driven by a constant pressure gradient or force. In the force-driven case, Poiseuille gas flow was studied both analytically and numerically by various methods, such as computational fluid dynamics, perturbation expansion (Tij and Santos, 1994), direct simulation Monte Carlo (DSMC) (Mansour et al., 1997; Zheng et al., 2002), Burnett solutions (Uribe and Garcia, 1999), super-Burnett solutions (Xu, 2003), entropic lattice Boltzmann method (Ansumali, 2004), a modified set of Navier-Stokes equations namely Brenner's hydrodynamic model (Guo and Xu, 2009), and molecular dynamics (MD). These studies revealed significant differences in the flow and thermal properties between high order models and conventional hydrodynamic theory results.

For example, the conventional hydrodynamic theory could not predict the peculiarities in Poiseuille flow, such as non-uniform pressure, local temperature minimum at the centerline, non-negligible tangential heat flux. The hydrodynamic theory predicts

temperature to be a maximum at the center where it should be a minimum. This indicates global failure which cannot be corrected by modifying transport coefficients or boundary conditions (Karniadakis et al., 2005).

Recently a non-classical theory based on a nonlinear coupled constitutive relation (called NCCR hereafter) was developed by Myong (2011) and shown to capture all these flow peculiarities in almost perfect agreement with DSMC data. The NCCR theory provides exact analytical solutions for the flow properties of Poiseuille gas flow, by considering rigorously the temperature dependence of viscosity and thermal conductivity, in terms of Knudsen number (Kn) and a dimensionless force parameter (ε_{h_w}); the two parameters which define a unique flow problem. The solutions were proved to exist for all ranges of Knudsen number and force parameter.

Molecular dynamics simulation of channel flow has been performed with soft-sphere potentials by Hannon et al. (1986) and Bhattacharya and Lie (1989) in which the flow peculiarities have not been emphasized. MD simulations have studied Poiseuille flow in narrow pores of few molecular diameters and have shown some differences for different pore widths. The deviation of MD velocity profile from that of continuum prediction was significant for channel widths smaller than 10 molecule diameters (Travis and Gubbins, 2000). These MD studies demonstrated that the conventional linear hydrodynamic theory fails for nanoscale flows.

The MD approach to solve micro/nano flows with the context of studying the flow peculiarities could provide deeper understanding of the flow and thermal physics. In this study, we attempt to study those peculiarities of force-driven Poiseuille flow, thermo-physical properties in particular, by molecular dynamics simulations and to compare them with the results provided by a recent non-classical hydrodynamic NCCR theory.

This paper is organized as follows: the flow conditions are defined in Section 2, the NCCR solutions for velocity, temperature and density are summarized in Section 3, MD simulation setup is described in Section 4, followed by results and discussion in Section 5 and finally the conclusions in Section 6.

2. Flow Conditions

A flow problem is defined uniquely by two non-dimensional parameters: Knudsen number (Kn) and a force related parameter ε_{h_w} (similar to Richardson number). The definition for the force parameter is given by

$$\varepsilon_{h_w} = \frac{ah}{RT_w} \tag{1}$$

where a is the external force which drives the flow, h is the channel height, R is the gas constant for a monatomic gas and T_w is the wall temperature. The same definition will be used in both MD and NCCR calculations.

The definition for Knudsen number used in NCCR solution is given by

$$\mathrm{Kn} = \sqrt{\frac{\pi}{2}}\frac{\eta_w\sqrt{RT_w}}{p_m h} \tag{2}$$

where η_w is the viscosity at the wall temperature and p_m is the pressure at the middle of the channel. In MD, the Knudsen number is defined as

$$\mathrm{Kn} = \frac{\lambda}{h} \tag{3}$$

where λ is the mean free path definition for hard sphere molecules given by,

$$\lambda = \frac{1}{\sqrt{2}\pi n d^2}. \tag{4}$$

Here n is the number density, d is the diameter of the molecule. These two dimensionless numbers (Kn and ε_{h_w}) together define a unique flow condition. In this study, the effect of rarefaction on the temperature profile is investigated by considering three different flow cases: $\mathrm{Kn} = 0.01$, 0.1 and 1.12 for $\varepsilon_{h_w} = 0.6$.

3. NCCR Solutions

The one dimensional force-driven compressible Poiseuille gas flow was analyzed

by Myong (2011) on the basis of nonlinear constitutive relation (NCCR) theory and a mathematical technique that considers rigorously the temperature dependence of viscosity and thermal conductivity. The new technique is based on the introduction of average quantities for velocity and temperature profiles, a spatial variable scaled by the temperature, and subsequent auxiliary relations. The solutions have been derived for all the flow properties in terms of Knudsen number (Kn) and force parameter (ε_{h_w}). The Maxwellian assumption of molecules was employed in the derivation. The solution for velocity is given as ($N_\delta = \sqrt{2\gamma/\pi}\, M$ Kn)

$$\frac{u^*}{u^*(0)} = 1 - \frac{T_w^*}{2u^*(0)} \frac{\varepsilon_{h_w}}{N_\delta} \cdot \left(\frac{\tan S^*}{2S_{1/2}^*} \right)^2 . \quad (5)$$

The solution for the temperature profile is given as trigonometric functions

$$\frac{T^*}{T^*(0)} = \cos^{-e} S^* \left(1 - \frac{\pi(\gamma-1)\Pr}{24\gamma(1-e/4)} \frac{T_w^{*5}}{T^*(0)} \cdot \frac{\varepsilon_{h_w}^2}{\mathrm{Kn}^2} \frac{F(S^*)}{(2S_{1/2}^*)^4} \right) \quad (6)$$

where $Tds = dy,\ y^* \equiv y/h,\ S^* \equiv \sqrt{2/3} T_w^* \varepsilon_{h_w} s^*,$ $s^* \equiv sT_r/h,\ e \equiv 3(\gamma-1)/(2\gamma)$. In the case of a monatomic gas, e is reduced to $3/5$. Here F is a function defined as

$$F(t) \equiv (4-e)\left[\frac{1}{(4-e)\cos^{4-e} t} - \frac{1}{(2-e)\cos^{2-e} t} - \left(\frac{1}{4-e} - \frac{1}{2-e} \right) \right]. \quad (7)$$

The function F is related to the quartic function in the Navier-Fourier solution as follows:

$$F(S^*) = (1-e/4)S^{*4} + O(S^{*6}).$$

The unknown value T_w^* in the equation (6), the average temperature, can be determined uniquely for given values of Kn and ε_{h_w} by solving the following algebraic equation using the bisection method:

$$\frac{\pi(\gamma-1)\Pr \varepsilon_{h_w}^2 T_w^{*5}}{384\gamma \mathrm{Kn}^2 (1-e/4)} \frac{F(S_{1/2}^*)}{S_{1/2}^{*4}} = T^*(0)\left(1-(1-\alpha_T)\cos^e S_{1/2}^*\right) - \alpha_T T_w^* \cos^e S_{1/2}^*,$$

$$\alpha_T = \frac{\bar{\beta}_T p_w^*}{1+\bar{\beta}_T p_w^*},\ \bar{\beta}_T = \frac{1}{4\omega_T \mathrm{Kn}}.$$

Finally, the density distribution across the channel is calculated using the equation of state,

$$\rho^*(s^*) = T^*(0)\frac{p^*}{T^*}, \quad (8)$$

where $p^*(S^*) = 1 + \tan^2 S^*$.

The detailed derivation of the analytical solutions can be found in Myong (2011). All the properties are non-dimensionalized with the corresponding reference (average or centerline, the channel height) values.

4. MD Simulation Setup

In this study, extensive MD simulations have been performed for the force-driven Poiseuille gas flows with LAMMPS (Large-scale Atomic/Molecular Massively Parallel Simulator). LAMMPS can be used as a parallel particle simulator at the atomic, meso, or continuum scale and it is distributed as an open source code by Sandia National Laboratories. As shown in Fig. 1, the fluid (Argon) atoms are confined between the two solid walls (Platinum) placed parallel to the flow direction (*x*-direction). Periodic boundary conditions are used in all the three directions. Each fluid atom is given a constant force in the *x*-direction to drive the flow throughout the simulation. Each wall is six layers thick and made of FCC (face centered cubic) crystal lattice.

The non-bonding interactions are modeled using Lennard-Jones (LJ) potential function given by

$$\phi(r) = \begin{cases} 4\varepsilon\left[\left(\frac{\sigma}{r} \right)^{12} - \left(\frac{\sigma}{r} \right)^{6} \right] & \text{for } r < r_c \\ 0 & \text{for } r > r_c \end{cases} \quad (9)$$

where ε is the depth of the potential well in LJ potential function, σ is the distance

parameter, r is the interatomic distance, and r_c is the cut-off distance beyond which the interactions are neglected. A cut-off distance of $r_c = 2.5\sigma$ is used in all the simulations. The LJ parameters of the atoms are given in Table 1 (Plimpton, 1995; Prabha and Sathian, 2013). The center of mass of the wall is maintained at a fixed position. The average temperature of the walls is regulated as constant at 300 K by Berendsen thermostat. However, the thermostat is not applied to the fluid atoms.

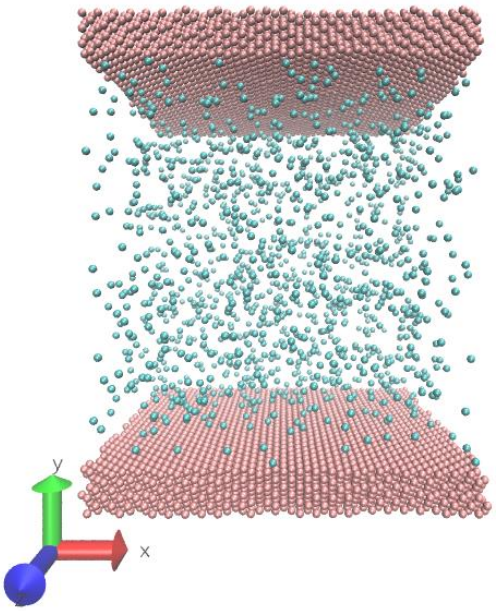

Fig. 1. MD simulation setup of Poiseuille gas flow between the two walls. The fluid atoms are driven by the force applied in *x*-direction.

Table 1
Lennard-Jones (LJ) interaction values for different pairs with their units given in brackets.

Interaction pair	σ (Å)	ε (kcal/mol)
Ar-Ar	3.4	0.238176
Pt-Pt	2.47	7.49808
Pt-Ar	2.94	0.157392

The numerical integrator used in LAMMPS is the velocity-Verlet algorithm with a time step of 1 femtosecond (fs). The channel dimension is $98\times100\times98$ Å^3 where the height of the channel is 100 Å for all the three cases but the number of fluid atoms is varied to obtain the desired Knudsen number (Kn). The force applied to each fluid atom to drive the flow is 0.003575 kcal/mol/Å, which is equivalent to a force parameter of $\varepsilon_{h_w} = 0.6$.

5. Results and Discussion

The thermal behavior of the force-driven Poiseuille gas flow is studied in comparison with the analytical solution by nonlinear coupled constitutive relation (NCCR) theory (Myong, 2011). The results are non-dimensionalized with respect to the values at the centerline for temperature, while the distance is non-dimensionalized with the channel height. The flow is defined uniquely by two non-dimensional parameters: Knudsen number (Kn) and a dimensionless force parameter (ε_{h_w}). Since we are interested in the effects of rarefaction on the temperature distribution of flow, we consider three different Knudsen numbers 0.01, 0.1, 1.12 for a fixed force parameter $\varepsilon_{h_w} = 0.6$.

The MD results across the channel are obtained by dividing the channel into a number of equally divided bins. The binned values are then time averaged for a number of time steps. The length of each bin in the y direction is Δy so that volume of each bin is the same. The number of bins used is 80 for Kn = 0.01 and 0.1 cases, and 32 for Kn = 1.12 case. The properties are averaged for all the atoms in each bin which results in a representative value for that bin. The dimension of the bin can be chosen at our choice (LAMMPS User's Manual, 2014). The density in each bin is then obtained by counting the mass of the total number of atoms in that bin divided by the volume of that bin and it is normalized with the value at the centerline. The results obtained by MD are compared with those of NCCR solutions. However, it should be noted that the MD simulations are performed using the argon atoms as fluid while the NCCR solution has been derived for Maxwell molecules.

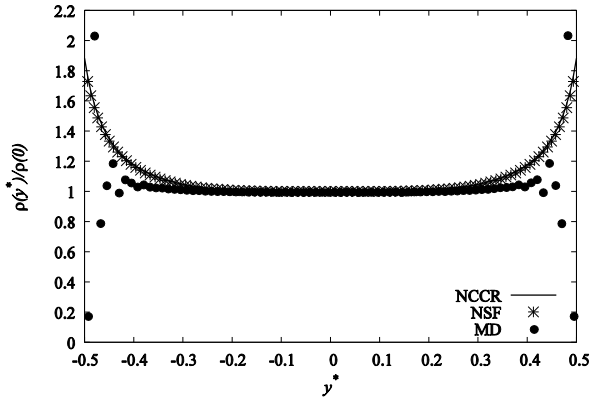

Fig. 2. Density profile across the channel for (Kn , ε_{h_w}) = (0.01, 0.6).

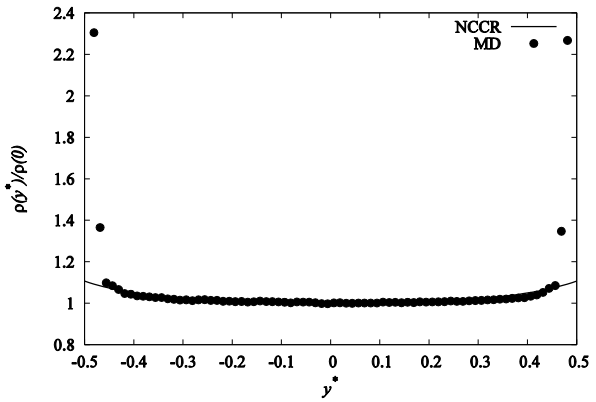

Fig. 3. Density profile across the channel for (Kn , ε_{h_w}) = (0.1, 0.6).

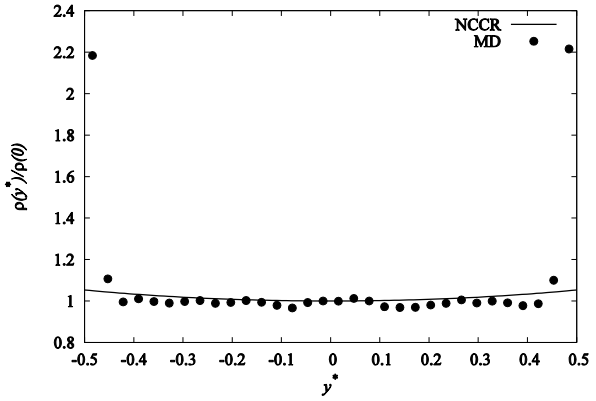

Fig. 4. Density profile across the channel for (Kn , ε_{h_w}) = (1.12, 0.6).

The MD density plots show qualitative agreement with NCCR data for all the three cases. As shown in Fig. 2 the oscillations near the wall in MD results are due to the atoms forming layers. As Knudsen number increases the layering effects decreases and we can observe less oscillation near the wall (Figs. 3 and 4). Though the discrepancy is seen near the wall, the agreement at the central region is good, especially for $\mathrm{Kn} = 0.1$ case (Fig. 3).

The streamwise velocity profile is also calculated by binning the velocity for all the atoms in each bin and then time averaged for a number of time steps. The MD velocity plots for $\mathrm{Kn} = 0.01$ and 0.1 cases (Figs. 5 and 6) show a better qualitative agreement with NCCR results.

At high Knudsen number 1.12, some discrepancy is found, as shown in Fig. 7, probably owing to the lesser number of atoms in the system. Some of gap may also be due to the difference in how to take into account the gas-wall molecular interaction. In the case of NCCR theory, the Langmuir slip model was used for the velocity slip and the temperature jump near the wall (Myong, 2011).

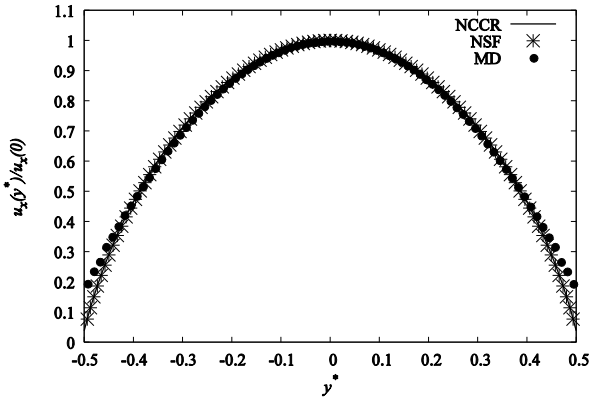

Fig. 5. Streamwise velocity profile across the channel for (Kn , ε_{h_w}) = (0.01, 0.6).

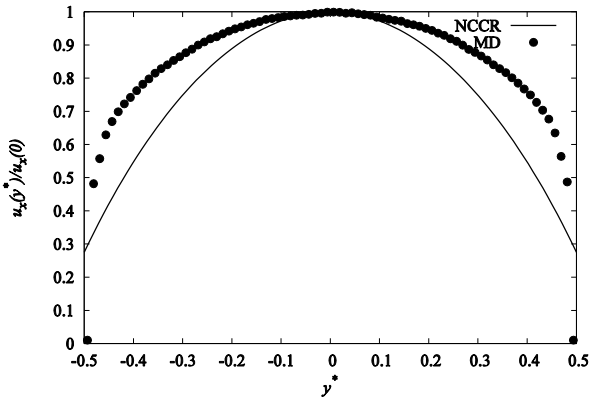

Fig. 6. Streamwise velocity profile across the channel for (Kn , ε_{h_w}) = (0.1, 0.6).

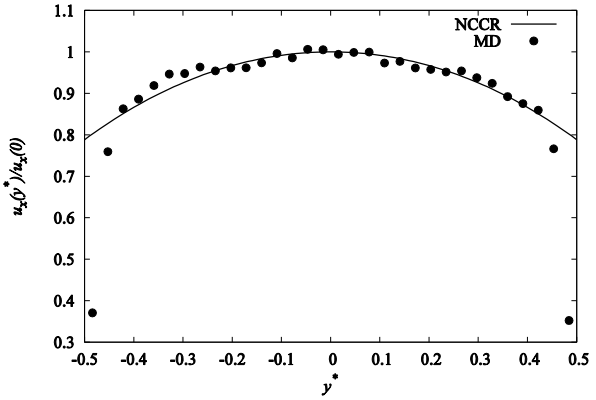

Fig. 7. Streamwise velocity profile across the channel for (Kn , ε_{h_w}) = (1.12, 0.6).

The temperature in each bin is measured from the total thermal kinetic energy for all the atoms in that bin. The binned temperature value is then time-averaged for a number of time steps and normalized with the centerline value. The expression for the temperature calculated by MD is then given as

$$\left\langle T\left(y_{bin}\right)\right\rangle = \frac{\left\langle \sum_{i\in bin}^{N_{bin}} m_i\left[\mathbf{v}_i - \mathbf{u}\left(y,t\right)\right]\left[\mathbf{v}_i - \mathbf{u}\left(y,t\right)\right]\right\rangle}{\left\langle 3N_{bin}k_B\right\rangle} \quad (10)$$

where m_i is the mass of the particle i, $\mathbf{v}_i$ is the total velocity of the particle i, $\mathbf{u}\left(y,t\right)$ is the instantaneous streaming velocity at y, N_{bin} is the number of atoms in that bin, k_B is the Boltzmann constant.

The existence of the central temperature minimum is clearly shown in Figs. 8-10.

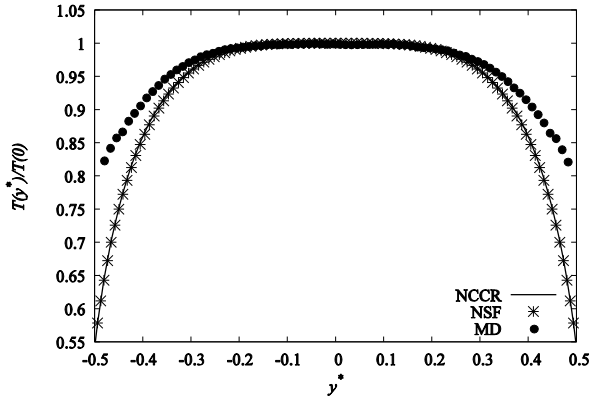

Fig. 8. Temperature profile across the channel for (Kn , ε_{h_w}) = (0.01, 0.6).

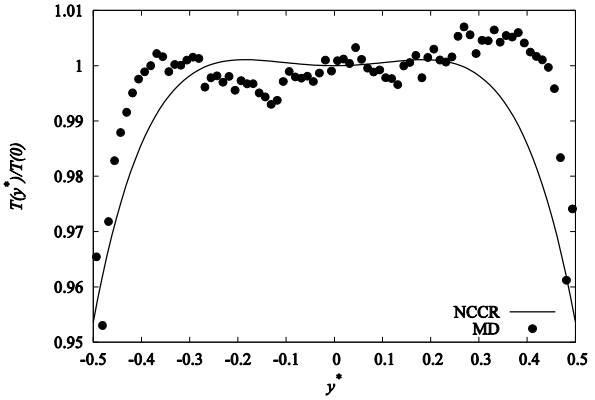

Fig. 9. Temperature profile across the channel for (Kn , ε_{h_w}) = (0.1, 0.6).

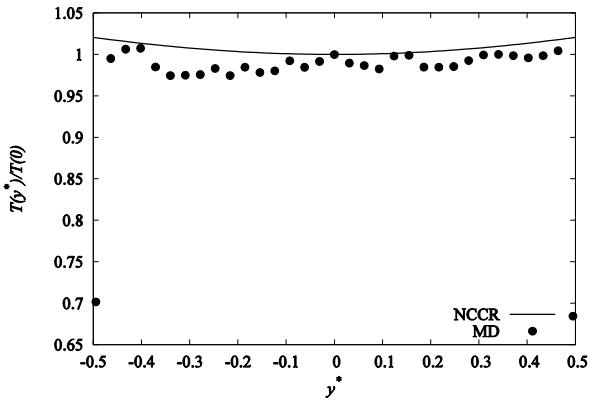

Fig. 10. Temperature profile across the channel for (Kn , ε_{h_w}) = (1.12, 0.6).

The MD temperature profile for (Kn , ε_{h_w}) = (0.01, 0.6) agrees well with the results of NCCR, as shown in Fig. 8. However some discrepancy can be observed near the wall. The local minimum in temperature at the central region is not well pronounced in this flow regime owing to small Knudsen number (Kn = 0.01). Also, the temperature in the central region is higher than that near the wall.

With increasing Knudsen numbers from 0.01 to 0.1 (see Figs. 9 and 10), the temperature minimum appears to be substantial. For Kn = 0.1, the local minimum is well pronounced with two off-center maxima as predicted by the theory. The temperature minimum in the NCCR theory occurs at the centerline due to the factor $\sec^e S^*$ in equation (6). This temperature minimum turned out to play a significant role in determining the mass flow rate (Myong,

2011). The MD data for ($\mathrm{Kn}, \varepsilon_{h_w}$) = (0.1, 0.6) also shows a qualitative agreement with NCCR theory. As shown in Fig. 10, the two maxima in the temperature profile move toward the walls reaching the boundaries when the Knudsen number is increased further from 0.1 to 1.12.

In all the three cases considered here, the density, velocity and temperature profiles predicted by MD showed a qualitative agreement with NCCR results. The channel dimension is maintained fixed and hence the number of fluid atoms used in the higher Knudsen number case is very low, leading to non-negligible noise in the results. Therefore the accurate calculation of the heat flux distribution for high Knudsen number flows in MD simulation remains a challenging subject. The thermal behavior analysis in terms of heat flux will be considered in the future works.

6. Conclusions

The thermal behaviors of the force-driven Poiseuille gas flows are studied by MD simulation method. In addition to the temperature distribution, density and velocity profiles are also considered. The results obtained using MD simulations were compared qualitatively with the results of non-classical NCCR theory. The NCCR theory provides fully analytical solutions for all the flow problems with respect to Knudsen number and force parameter. It also explains the occurrence of the local minimum and maxima in the temperature profile in concise way.

The qualitative assessment of the MD results has been undertaken by non-dimensionalizing the properties with the corresponding centerline values. The effects of rarefaction on the flow and thermal behaviors of force-driven Poiseuille gas flow are examined by considering three different Knudsen numbers (Kn = 0.01, 0.1, 1.12) for the same external driving force. The results provided by MD seem to agree qualitatively well with those of NCCR theory. For all the three cases considered here, the present MD results show a qualitative agreement with NCCR predictions. At the same time, some deviations were found, which might be attributed to the different fluid atoms and different treatment of gas-wall molecular interaction employed in MD and NCCR.

The estimation of the thermal properties of Poiseuille gas flow may be relevant to the analysis of the cooling system of MEMS/NEMS devices. It is because the thermal behavior will determine the effectiveness of the cooling system and the mas flow rate is significantly influenced by the temperature distribution. In this study, the thermal behaviors of force-driven Poiseuille gas flow were analyzed in detail in terms of temperature profiles and a qualitative agreement between MD and non-classical NCCR theoretical results was demonstrated.

The analysis of other peculiarities of force-driven compressible Poiseuille gas flow such as non-negligible tangential heat flux is being actively undertaken at present and will be reported in near future.

Acknowledgement

This work was supported by the National Research Foundation of Korea funded by the Ministry of Education, Science and Technology (Basic Science Research Program NRF 2012-R1A2A2A02-046270 and Priority Research Centers Program NRF 2009-009414), South Korea.

References

Ansumali, S., 2004. Minimal Kinetic Modeling of Hydrodynamics. Doctor of Technical Sciences Dissertation, Swiss Federal Institute of Technology Zurich.

Bhattacharya, D.K., Lie, G.C., 1989. Molecular-Dynamics simulations of nonequilibrium heat and momentum transport in very dilute gases. Phys. Rev. Lett. 62, 897.

Guo, Z., Xu, K., 2009. Numerical validation of Brenner's hydrodynamic model by force driven Poiseuille flow. Adv. App. Math. Mech. 1, 391-401.

Hannon, L., Lie, G.C., Clementi, E., 1986. Molecular dynamics simulation of channel

flow. Phys. Lett. A, 119, 174.

Karniadakis, G., Beskok, B., Aluru, N., 2005. Microflows and Nanoflows, Fundamentals and Simulation. Springer.

LAMMPS User's Manual, 2014. http://lammps.sandia.gov – Sandia National Laboratories.

Mansour M.M., Baras, F., Garcia, A.L., 1997. On the validity of hydrodynamics in plane Poiseuille flows. Physica A 240, 255.

Myong, R.S., 2011. A full analytical solution for the force-driven compressible Poiseuille gas flow based on a nonlinear coupled constitutive relation. Phys. Fluids 23, 012002.
doi: 10.1063/1.3540671
http://acml.gnu.ac.kr/e-home/index.htm (03/2014)

Plimpton, S.J., 1995. Fast parallel algorithms for short-range molecular dynamics. J. Comput. Phys. 117, 1-19.

Prabha, S.K., Sathian, S.P., 2012. Determination of accommodation coefficients of a gas mixture in a nanochannel with molecular dynamics. Micro. Nanofluid 13, 883-890.
doi: 10.1007/s10404-012-1020-9

Prabha, S.K., Sathian, S.P., 2013. Calculation of thermo-physical properties of Poiseuille flow in a nano-channel. Int. J. Heat Mass Trans. 58, 217-223.

Tij, M., Santos, A., 1994. Perturbation analysis of a stationary nonequilibrium flow generated by an external force. J. Stat. Phys. 76, 1399.

Travis, K.P., Gubbins, K.E., 2000. Poiseuille flow of Lennar-Jones fluids in narrow slit pores. J. Chem. Phys. 112, 1984.

Uribe, F.J., Garcia, A.L., 1999. Burnett description for plane Poiseuille flow. Phys. Rev. E. 60, 4063-4078.

Xu, K., 2003. Super-Burnett solutions for Poiseuille flow. Phys. Fluids 15, 2077.
doi: 10.1063/1.1577564

Zheng, Y., Garcia, A.L., Alder, B.J., 2002. Comparison of kinetic theory and hydrodynamics for Poiseuille flow. J. Stat. Phys. 109, 314.